Left Ventricle wall extraction in cardiac MRI using region based level sets and vector field convolution

Conference Paper · July 2015

DOI: 10.1109/IWOBI.2015.7160156

CITATION
1

READS
27

7 authors, including:

Anupama Bhan
Amity University
22 PUBLICATIONS **57** CITATIONS
SEE PROFILE

Ayush Goyal
Texas A&M University - Kingsville
54 PUBLICATIONS **197** CITATIONS
SEE PROFILE

Carlos M. Travieso
Universidad de Las Palmas de Gran Canaria
374 PUBLICATIONS **2,788** CITATIONS
SEE PROFILE

Jesús B. Alonso
Universidad de Las Palmas de Gran Canaria
282 PUBLICATIONS **2,599** CITATIONS
SEE PROFILE

Left Ventricle Wall Extraction in Cardiac MRI Using Region Based Level sets and Vector field Convolution

Anupama Bhan, Ayush Goyal, Malay Kishore Dutta
Dushyant Sankhla, Pankhuri Khanna
Amity School of Engineering & Technology
Amity University, Noida, India
abhan@amity.edu, aja.govinda@gmail.com

Carlos M. Travieso, Jesús B. Alonso Hernández
Signal and Communications Department
University of Las Palmas de Gran Canaria,
Las Palmas de Gran Canaria, Spain
carlos.travieso@ulpgc.es,jb.alonsohernandez@gmail.com

Abstract — Left Ventricle imaging using short-axis MRI sequences is considered as an important tool used for evaluating cardiac function by calculating important clinical cardiac parameters. This requires manual tracing of LV wall which is subjective, tedious and time-consuming process. This paper presents semi-automatic method for left ventricle inner wall (endocardium) segmentation. This paper focuses on segmenting one complete cardiac cycle without any user intervention. The method used in this paper is region based level sets and vector field convolution active contour model out of which the later method has significantly achieved the better segmentation results. The end systolic and end diastolic volume is calculated by both the methods. The methods are tested on many images and time consumption is reduced using vector field convolution which takes only 30 iterations for segmenting one image per slice. The clinical parameters end diastolic volume, end systolic volume and ejection fraction values obtained from both methods are compared with the values of manually segmented images. The value obtained from vector field convolution gives a closer value to manual segmentation which proves the accuracy of the method and can be considered clinically significant. This semi-automatic approach provides cardiac radiologists a practical method for an accurate segmentation of left ventricle.

Keywords – Cardiac MRI; Segmentation; Endocardium; Level sets; Vector Field Convolution Model.

I. INTRODUCTION

Cardiovascular diseases occupied 33.7% in the death chart generated by UN in 2011, whereas cancer accounted for 12.5% deaths. By 2020 heart diseases would touch the top of the death rate chart.[1] The alarming situation accelerates the urgency to detect cardiovascular diseases before time, accurately with reduced time consumption. Since left ventricle performs the task of pumping blood, it is of a particular interest to most of the radiologists. A number of challenges have been encountered while segmenting left ventricle. The segmentation is divided into three categories- low level segmentation: histogram and threshold segmentation techniques, medium level segmentation: edge based segmentation and high level segmentation: active contour or deformable models [2][3]. This paper concentrates on the region based segmentation combining level set for extraction of LV inner wall and active contour model which uses vector field convolution as its external force. Global threshold [4] and region based segmentation [5] is used to segment mask for endocardium and level set model uses this threshold image as an initial mask for extraction of LV wall. In Active contour model [6][7] Vector Field Convolution was used as an external force due to its wide capture range and more accuracy around concavities.

The main contribution of the paper is to extract the outer wall of left ventricle in cardiac MRI using vector field convolution technique which strategically improves the accuracy of the system as compared to traditional region based level set technique. The calculated values obtained from both the techniques for End diastolic, End systolic and ejection fraction of normal and abnormal subject are compared with the ground truth. It concludes that Vector field convolution technique gives better results than traditional level set keeping manual segmentation values as reference.

Rest of the paper is organized as follows: section II presents flow chart of Region based level set, section III discusses the extraction of endocardium with Vector field convolution. The experimental results are shown in section IV. This section also includes various graphs to depict the comparison between two methods with the ground truth. Section V concludes the paper.

II. METHODOLOGY

A. REGION-BASED SEGMENTATION

Segmenting the left ventricle depends on segmenting two different contours, interior contour is endocardium that surrounds the left ventricle blood pool and eternal contour is epicardium. For segmenting endocardium, the problem is gray value inhomogenieties inside the LV cavity itself. In region based method, global threshold is used as an initial step to form a base for region based segmentation which involves using the segmented Epicardium as the mask for extracting Endocardium. Level sets uses the mask as as initial pointer from which it is converged onto the Endocardium boundary. These steps are repeated for all the

frames of the MRI and the endocardium areas are plotted against Frames. End Diastolic volume, End Systolic Volumeand Ejection Fraction has been calculated by multiplying the Endocardium Area during ED and ES by slice thickness. [8]

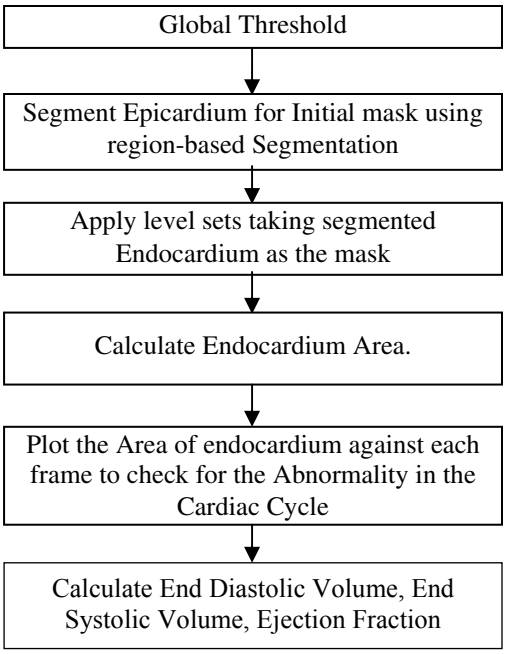

Fig.1: Flow Chart of Regional Segmentation

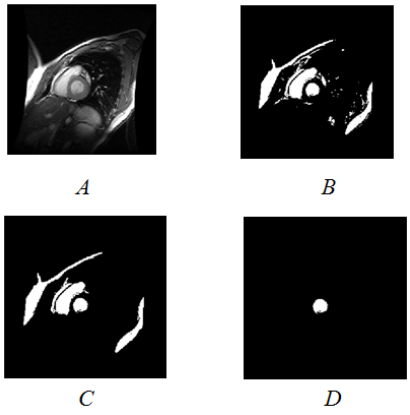

Fig.2: Region-Based Segmentation of Epicardium
A. Original MRI Image
B. Binary Image
C. After refining the image to minimum regions
D. The Segmented Ventricle

Segmentation involves separating an image into regions (or their contours) corresponding to objects. It has been tried to segment regions by identifying common properties. Or identifying contours by identifying differences between regions (edges). Intensity is the simplest property pixels of a particular region share. Therefore, a natural way to segment such regions is through thresholding as shown in Fig2.
If g(x, y) is a threshold version of f (x, y) at some global threshold T. g is equal to 1 if f (x, y) ≥ T and zero otherwise. Pixels that belong to an object are denoted with 1 / true while those pixels that are the background are 0 / false.

B. Traditional level set algorithm

This method begins with a contour in the image plane defining an initial segmentation, and then evolves the contour according to evolution equation (1). The goal is to evolve the contour in such a way that it stops on the boundaries of the foreground region.
It defines some function φ(i, j, t) (the level-set function), where (i, j) are coordinates in the image plane and t is an artificial "time." At any given time, the level set function simultaneously defines an edge contour and a segmentation of the image. The edge contour is taken to be the zero level set {(i, j) s.t. φ(i, j, t) = 0}, and the segmentation is given by the two regions {φ > 0} and {φ < 0}.
It uses Variational calculus methods to evolve the level set function. The methods work by seeking a level set function that minimizes some functional.[9][10] The goal is to evolve the contour in such a way that it stops on the boundaries of the foreground region In this context, functional means a mapping that takes a level set function φ as input, and returns a real number as shown in Fig 4. The problem is then to seek a function φ that is a critical point (minimum or maximum) of this functional. The main concern is coming up with a functional whose critical points are level sets that give useful segmentations for a given problem.
The goal of the level set algorithm is to minimize this fitting energy for a given image, and the minimizing level set function φ will define the segmentation. In its most general form, the fitting energy is

$$F(\emptyset) = \mu\left(\int_{\Omega 1}^{\Omega 2} c\,|\nabla H\,(\emptyset)|dx\right) + \nu\int_{\Omega 1}^{\Omega 2} H(\phi)dx + \lambda 1\Omega 1\Omega 2I - C1 \quad H \quad (\phi)dx + \lambda 2\int_{\Omega 1}^{\Omega 2}(I - C2)(1 - H\,(\phi))dx \tag{1}$$

Where μ, ν, λ1, λ2 and p are parameters selected by the user to fit a particular class of images. c1 and c2 are the averages of the image I in the regions where φ > 0 and φ < 0 respectively. The drawback of this method is reinitializing the Level Set Function. It is necessary at each iteration to rescale the level set function to keep it from becoming too flat. Endocardial boundaries are automatically detected by applying a region-based level set segmentation which drives the curve evolution towards the homogenous region which have different local noise patterns. The same process is then repeated for all slices from base to apex. The clinical parameters calculated are shown in Table I and II.

III. *SEGMENTATION BY VECTOR FIELD CONVOLUTION*

This model is also popularly known as deformable model is more promising than traditional region based level sets as its ability to lock to the target boundary with minimum number of iterations and it yields closer values of clinical parameters to standard reference values.

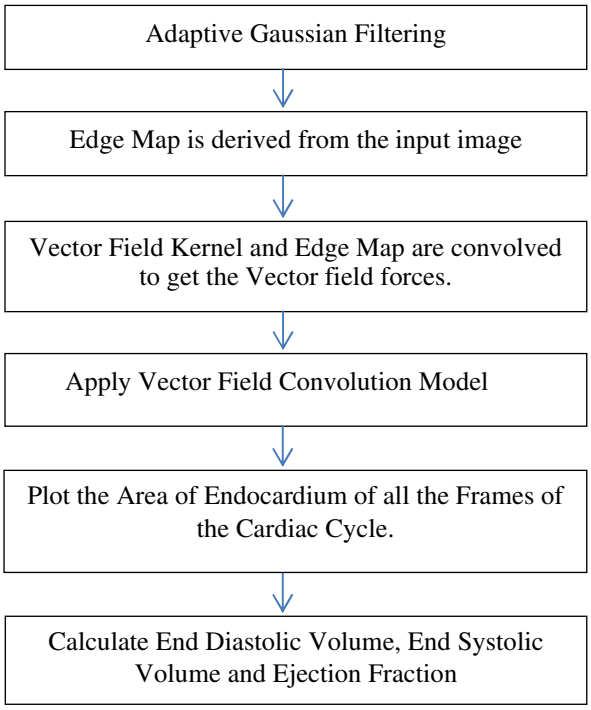

Fig.3: Flow Chart of Vector Field Convolution

A. Adaptive Gaussian Filtering:

The two-dimensional digital Gaussian filter can be expressed as:

$$G(x,y) = \frac{1}{\sqrt{2\pi\sigma}} exp^{\frac{-(x^2+y^2)}{2\sigma^2}} \quad (2)$$

Where, $(\sigma)^2$ is the variance of Gaussian filter, and the size of the filter kernel is often determined according to the amount of smoothness required in the image to eliminate the high frequency components and x and y are spatial coordinates. When Global Gaussian Filter is used for noise suppression, a large filter variance is effective in smoothing the image, but noise reduction comes with a trade-off that it makes the edges distorted. It also gives rise to edge position displacement, the vanishing of edges, and phantom edges as shown in Fig.5. The basic method to solve these problems is that, the pre-processing of an image is done using different filters with different filter variances, and then detecting edges in these filtered images. The final edge detection result is a generation of the edge images by certain thresholds that determine whether the abrupt change in the pixel is phantom edge or real edge. The filter is used to prevent the locking of active contour around the artefacts inside the Endocardium. This produces an accurate edge map. The calculation of the external force can be broken down to two independent steps: the formation of edge map from the image, and the computation of the external force from the edge map. Although the quality of the edge map is a critical factor in snake performance. The static forces are those that are calculated from the image, and remain unchanged as the snake deforms. The static forces can be further classified based on the force sources. Edge-based static forces are calculated from the image edges, whereas region-based static forces are computed using the region intensity and/or texture information.

B. Vector Field Convolution

The active models deform on the image domain and capture a desired feature by minimizing energy functional subject to certain constraints.[11] The energy functional usually contains two terms: an internal energy, which constrains the smoothness and tautness of the model, and an external energy, which attracts the elastic model. An active contour is a parametric curve represented by

$$\mathrm{v}(s) = [x(s), y(s)]^T, s\epsilon[0,1] \quad (3)$$

That deforms across the image to minimize the energy functional.

$$E_{ac} = \int_0^1 \left[\frac{1}{2}(\alpha|v'(s)|^2 + \beta|v''(s)|^2) + E_{ex}(v(s))\right] ds \quad (4)$$

Where α and β are parameters that represent the degree of the smoothness and rigidity of the contour, respectively, and v' and v'' are the first and second derivatives of **v(s)** with respect to s. E_{ext} denotes the external energy, the value of which is minimum at the ROI .

In Vector field convolution, active contours use the Vector field as the external force [4]. The standard external force $f_{ext}(v)$ where $f_{ext} = -\nabla E_{ext}(v)$ is replaced by the VFC field $f_{vfc}(v)$.

Static external forces called *vector field convolution* (VFC) is introduced in this section. A *vector field kernel*

$$\mathrm{K}(x,y) = [u_k(x,y), v_k(x,y)] \quad (5)$$

is first defined, in which all the vectors point to the kernel origin

$$\mathrm{k}(x,y) = \mathrm{m}(x,y)\mathrm{n}(x,y) \quad (6)$$

Where, m(x,y) is the magnitude of the vector at (x,y) and n(x,y) is the unit vector pointing to the kernel origin (0,0).

If the origin is the ROI, the vector field kernel has the desirable property that a free particle placed anywhere in the field is able to move to the ROI, such as edges. Calculating the convolution of the vector field kernel and the edge map generated from the image gives the VFC external field. As shown in Fig. 7 and Fig. 8. Since the edge map is non-negative and larger near the image edges, edges are more

predominant than homogeneous regions to the VFC. Therefore, free particles in VFC external field [12] are attracted more to edges. The VFC field overcomes the problem because strong edges contribute more to the VFC field than weak edges and noise.

The static forces are those that are calculated from the image, and remain unchanged as the snake deforms. The static forces can be further classified based on the force sources. Edge-based static forces are calculated from the image edges, whereas region-based static forces are computed using the region intensity and/or texture information. As the active contour nears the edge the magnitude of the vector field decreases along a positive function. Once the snake contour is initialized, it does not requires any user intervention to segment rest of the images in a cardiac cycle as shown in Fig. 9. The VFC snakes have not only a large capture range and ability to capture concavities, but also better robustness to noise and initialization, flexibility of tailoring the force field, and reduced computational cost as it takes only 30 iterations per slice.

IV. EXPERIMENTAL RESULTS

The method has been tested on datasets published by the MICCAI 2009 Left Ventricular segmentation Grand Challenge workshop [12] which has been made available by Sunnybrook Health Science Centre.

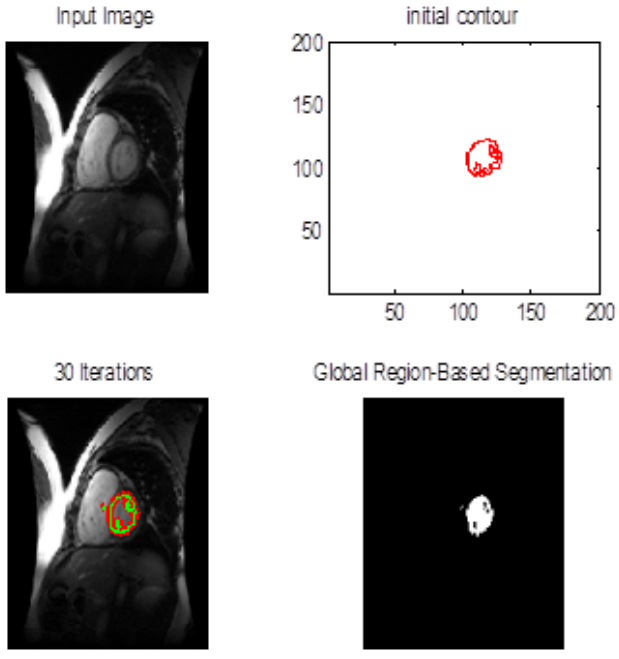

Fig.4: Segmentation of the Endocardium Wall

Fig.4 shows the results of the region based segmentation which segments outer wall of LV and takes it as an initial mask by level set evolution to segment inner wall of LV.

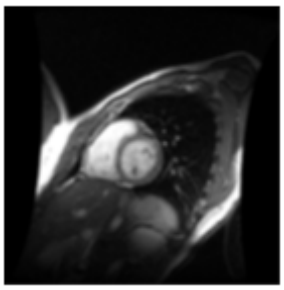

Fig.5: Gaussian filtered image

Fig. 5 shows the Gaussian filtered image used as a pre processing step for smoothing

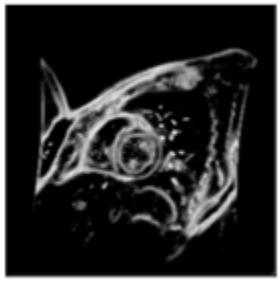

Fig.6: Edge Map

Fig. 6 shows the edge map which is convolved with vector field

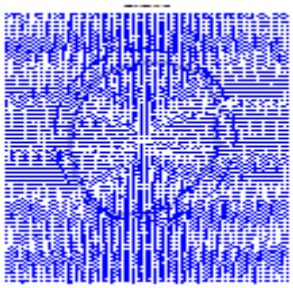

Fig.7: Vector fields

Fig. 7shows Normalized vector field which helps to push contour towards endocardium wall.

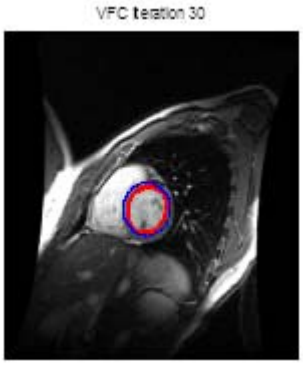

Fig.8: Segmented Endocardium, Blue - Deformed snake
Red - Initial mask

Fig. 8 shows the segmented endocardium

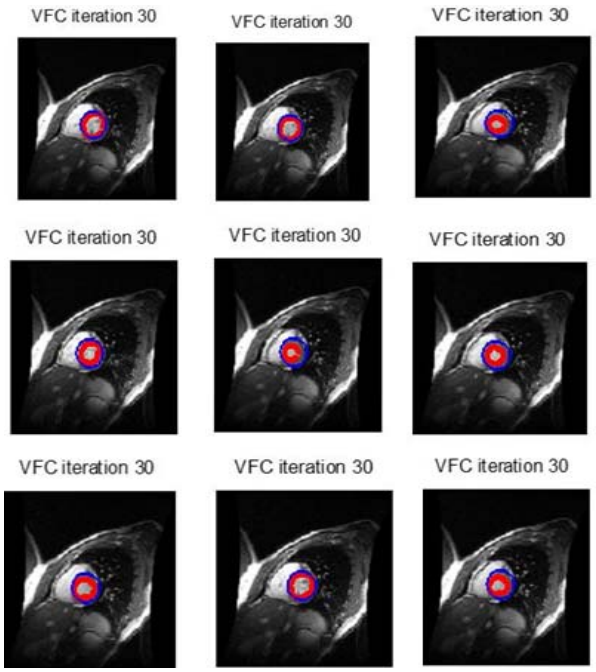

Fig.9: Segmented Endocardium of a Cardiac Cycle

Fig. 9 shows segmented endocardium of one complete cardiac cycle

The process takes 14 seconds per frame to complete the envelope process. The clinical parameters are calculated using equation 6:

$$Ejection\ Fraction = \frac{Diastolic\ Volume - Systolic\ Volume}{Diastolic\ Volume} \quad (7)$$

Table I: Table of Ejection Fractions of Both methods-(RB: Region Based Method; VFC: Vector Field Convolution algorithm).

Method	Diastolic Volume(mm^3)	Systolic Volume (mm^3)	Ejection Fraction
$RB_{Abnormal}$	10426.653	5040.936	0.5165
RB_{Normal}	11294.55	4742.39	0.5801
$VFC_{Abnormal}$	11722.554	5138.69	0.5254
VFC_{Normal}	12932.59	5564.052	0.6333

Table II: *Table of Ejection Fraction of the Ground Truth(Manual segmentation)*

Method	Diastolic Volume (mm^3)	Systolic Volume (mm^3)	Ejection Fraction
$Manual_{Abnormal}$	12156.1	5617.0863	0.537856
$Manual_{Normal}$	133227.88	5511.615	0.583333

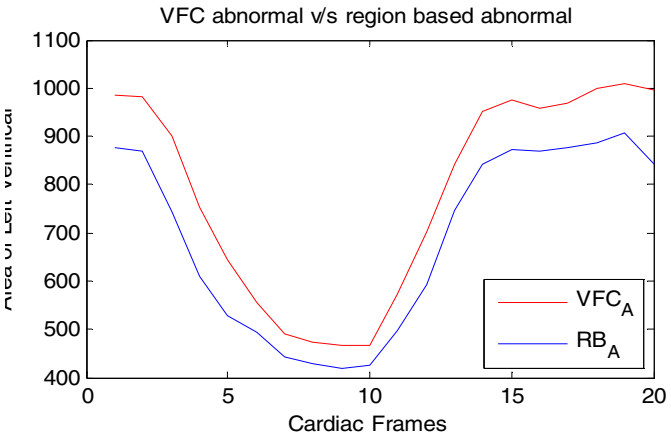

Fig.10: Graph of abnormal VFC Cycle vs abnormal Region Based Cycle (RB_A: Output by Region Based Segmentation of an Abnormal Patient), (VFC_A: Vector Field Convolution of an Abnormal Patient)

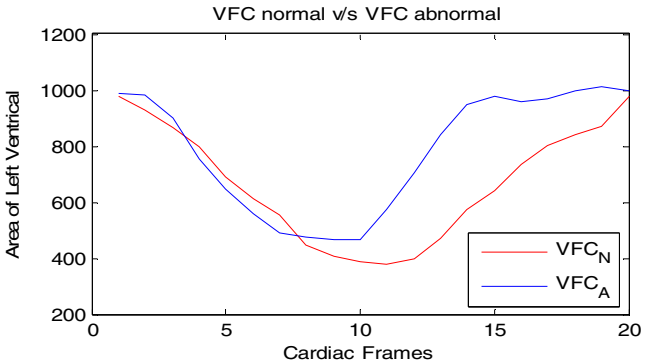

Fig.11: Graph of normal VFC Cycle vs abnormal VFC Cycle (VFC_A: Output by Vector Field Convolution of an Abnormal Patient), (VFC_N: Vector Field Convolution of a Normal Patient)

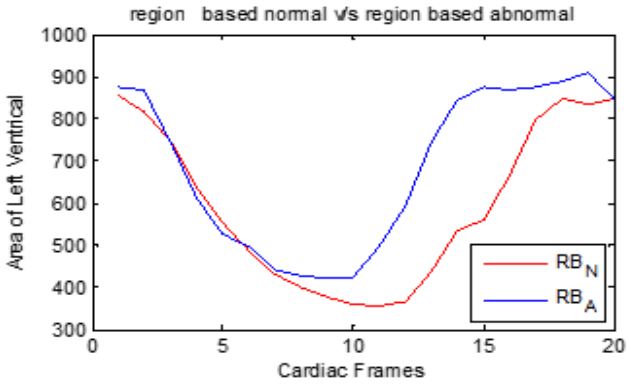

Fig.12: Graph of normal Region Based Cycle vs abnormal Region Based Cycle (RB_N: Output by Region Based Segmentation of a Normal Patient, RB_A: Output of Region Based Segmentation of an Abnormal Patient)

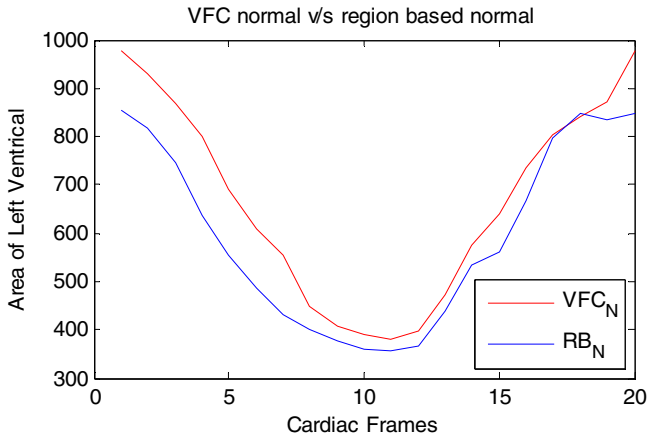

Fig.13: Graph of normal VFC Cycle vs normal Region Based Cycle (RB_N: Output by Region Based Segmentation of an Normal Patient), (VFC_N: Vector Field Convolution of a Normal Patient)

The graphs plotted in Fig. 11 shows the cardiac cycle output for systolic and diastolic phase for normal and abnormal subject using vector field convolution model. Fig. 12 shows the comparison of region based level set vs. VFC of normal subject. Fig. 13 shows the graph of VFC and region based for normal subject. It can be seen VFC gives more systolic and diastolic value in terms of area of LV inner wall.

V. CONCLUSION AND FUTURE WORK

It can be noted that the shape of the abnormal and normal Cardiac Cycle of both the methods, is similar, showing the need of a ground truth value to determine the efficiency of the same. The values of clinical parameters are validated from the manually segmented images from expert radiologists which is available with all details in the database.

The varied range of outputs can be accounted to the varying intensities of the MRI, as the experiment was observed for multiple patients but careful input with doctors can be very productive even with these errors. The above graphs depict the plot of the endocardium area versus frames. It is observed that the normal cardiac cycle forms a parabola whereas abnormal cardiac cycle forms a distorted one.
After the calculation, it is observed that the Ejection Fraction is < 55% for any Abnormal Cardiac Cycle and between 55% - 70% for any Normal Cardiac Cycle.
The shape of Abnormal and Normal Cardiac plot is also a clear indicator of the efficiency of the heart to function properly. The Future work will extend the segmentation of endo and epi cardium on a same frame to reduce manual segmentation.

REFERENCES

[1] G. Eason, B. Noble, and I. N. Sneddon, “On certain integrals of Lipschitz-Hankel type involving products of Bessel functions,” Phil. Trans. Roy. Soc. London, vol. A247, pp. 529–551, April 1955. *(references)*

[2] J. Clerk Maxwell, A Treatise on Electricity and Magnetism, 3rd ed., vol. 2. Oxford: Clarendon, 1892, pp.68–73.

[3] I. S. Jacobs and C. P. Bean, “Fine particles, thin films and exchange anisotropy,” in Magnetism, vol. III, G. T. Rado and H. Suhl, Eds. New York: Academic, 1963, pp. 271–350.

[4] K. Elissa, “Title of paper if known,” unpublished.

[5] R. Nicole, “Title of paper with only first word capitalized,” J. Name Stand. Abbrev., in press.

[6] Y. Yorozu, M. Hirano, K. Oka, and Y. Tagawa, “Electron spectroscopy studies on magneto-optical media and plastic substrate interface,” IEEE Transl. J. Magn. Japan, vol. 2, pp. 740–741, August 1987 [Digests 9th Annual Conf. Magnetics Japan, p. 301, 1982].

[7] M. Young, The Technical Writer’s Handbook. Mill Valley, CA: University Science, 1989.

[8] D. Terzopoulos, A. Witkin, and M. Kass, “Constraints on deformable models-recovering 3D shape and nonrigid motion,” Artif. Intell., vol. 36, pp. 91–123, 1988.

[9] M. Gastaud, M. Barlaud, and G. Aubert, “Combining shape prior and statistical features for active contour segmentation,” IEEE Trans. Circuits Syst. Video Technol., vol. 14, no. 5, pp. 726–734, May 2004.

[10] J.-O. Lachaud and A. Montanvert, “Deformable meshes with automated topology changes for coarse-to-fine three-dimensional surface extraction,” Med. Image Anal., vol. 3, pp. 187–207, 1999.

[11] T. McInemey and D. Terzopoulos, “Topology adaptive deformable surfaces for medical image volume segmentation,” IEEE Trans. Med. Imag., vol. 18, no. 10, pp. 840–850, Oct. 1999.

[12] T. McInerney and D. Terzopoulos, “A dynamic finite element surface model for segmentation and tracking in multidimensional medical images with application to cardiac 4D image analysis,” Comput. Med. Imag. Graph., vol. 19, pp. 69–83, 1995.

[13] N. Ray and S. T. Acton, “Motion gradient vector flow: An external force for tracking rolling leukocytes with shape and size constrained active contours,” IEEE Trans. Med. Imag., vol. 23, no. 12, pp. 1466–1478, Dec. 2004.

[14] N. Ray, S. T. Acton, and K. Ley, “Tracking leukocytes in vivo with shape and size constrained active contours,” IEEE Trans. Med. Imag., vol. 21, no. 10, pp. 1222–1235, Oct. 2002.

[15] A. R. Mansouri, D. P. Mukherjee, and S. T. Acton, “Constraining active contour evolution via lie groups of transformation,” IEEE Trans. Image Process., vol. 13, no. 6, pp. 853–863, Jun. 2004.

[16] N. Paragios and R. Deriche, “Geodesic active contours and level sets for the detection and tracking of moving objects,” IEEE Trans. Pattern Anal. Mach. Intell., vol. 22, no. 3, pp. 266–280, Mar. 2000.

[17] T. F. Cootes, G. J. Edwards, and C. J. Taylor, “Active appearance models,” IEEE Trans. Pattern Anal. Mach. Intell., vol. 23, no. 6, pp. 681–685, Jun. 2001.

[18] T. F. Cootes, C. J. Talyor, D. H. Cooper, and J. Graham, “Active shape models—Their training and applications,” Comput. Vis. Image Understand., vol. 61, pp. 38–59, 1995.

[19] C.Feng,C.Li, D.Zhao and H.Litt, “Segmentation of left ventricle using Two-Layer Level Set Approach,” Medical Image Computing and Computer-Assisted Intervention-MICCAI 2013, 477-484.